

Figure S1. Description of vascular phenotypes. **A.** DIC images showing xylem morphology in different regions (1-4) of a 5-day-old Arabidopsis root, from a distance above the root apical meristem to the hypocotyl. At the rootward end, the stele consists of a xylem axis with two differentiated protoxylem (p) strands in the periphery and two metaxylem (m) strands in the middle (1). This pattern continues shootward (1) until a third metaxylem strand differentiates in the central part of stele (3) forming a fully differentiated xylem axis with two protoxylem and three metaxylem (4) (sometimes four) strands, a pattern that continues until the hypocotyl. **B** and **C.** Under low ABA biosynthesis or signalling conditions, breaks in xylem strands were observed. Shown here are representative images of a longer (**B**) and shorter metaxylem strand break (**C**) in *aba2-1*. Zoomed in images in **B** represent different parts of the shown root numbered from the root-ward end. Here, the pattern is wt-like with two protoxylem and two metaxylem strands (1). This pattern continues (2) but one metaxylem stand stops (3) creating a discontinuous metaxylem strand (4 and 5). Higher up in the root, the xylem pattern is again wt-like (6). **D.** Representative images of vascular phenotypes that occur as a result of exogenous ABA treatment (0.5μM). Images 1-5 show different regions of the same root. Characteristic xylem morphological changes caused by high ABA levels include: change in the secondary cell wall of metaxylem from pitted to reticulate (1), formation of the central metaxylem strand at considerably lower point in the root compared to wt (2), occurrence of double protoxylem strands (4 and 5) i.e. an ectopic protoxylem strand either at an angle relative to the ordinary protoxylem strand or an ectopic protoxylem strand that occurs in metaxylem position indicating an identity shift from metaxylem to protoxylem. Image 6 represents the wt xylem pattern prior to the ABA treatment. Scale bars: 15μm.

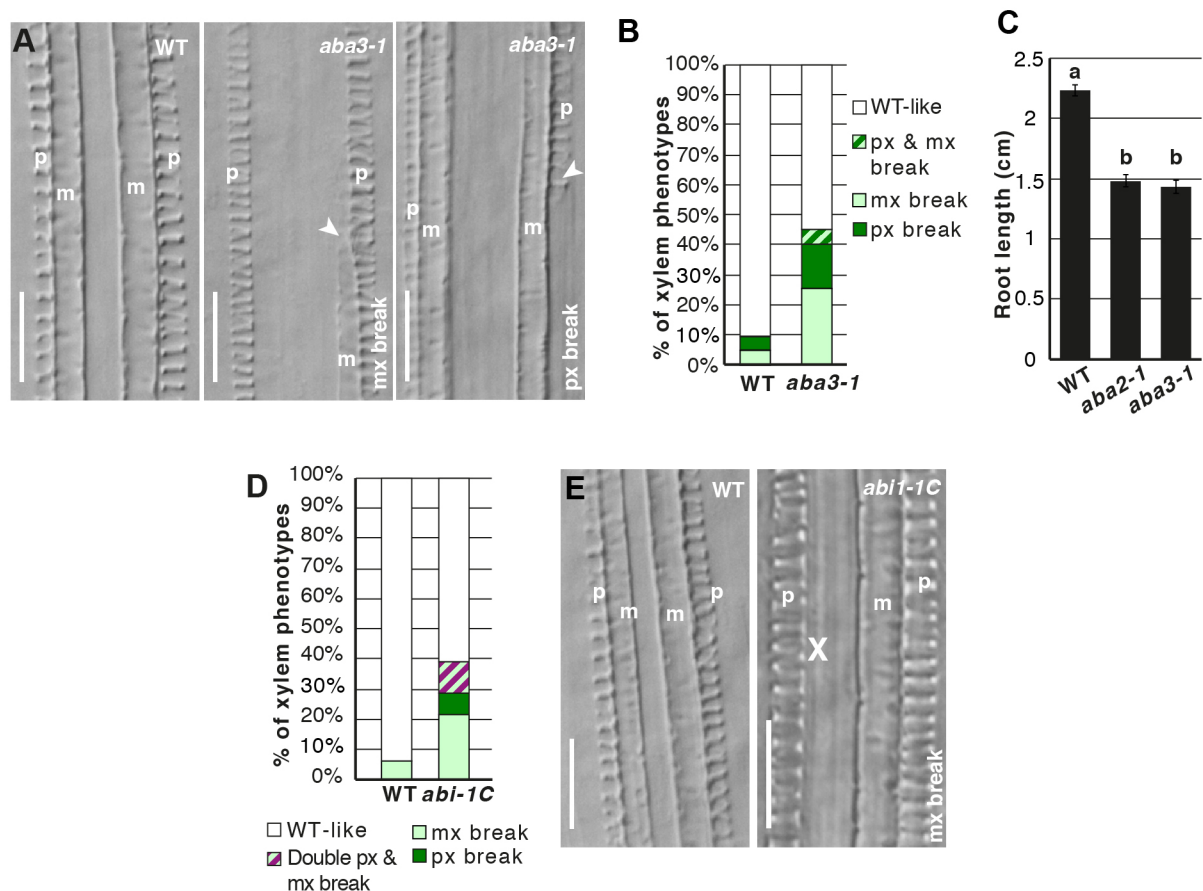


Figure S2. Xylem defects in ABA biosynthesis and signalling mutants. **A.** DIC images of *aba3-1* mutants and wt. **B.** Quantification of xylem phenotypes in *aba3-1* compared to wt (wt, n=19; *aba3-1*; n=11). **C.** Root length measurements of wt (n=37), *aba2-1* (n=41) and *aba3-1* (n=20) 5 days after germination. a and b represent significant differences by Tukey's pairwise comparison. **D.** Quantification of xylem phenotypes in *abi1-1C* compared to wt. **E.** DIC images of wt and *abi1-1C*. Scale bars: 15 μ m.

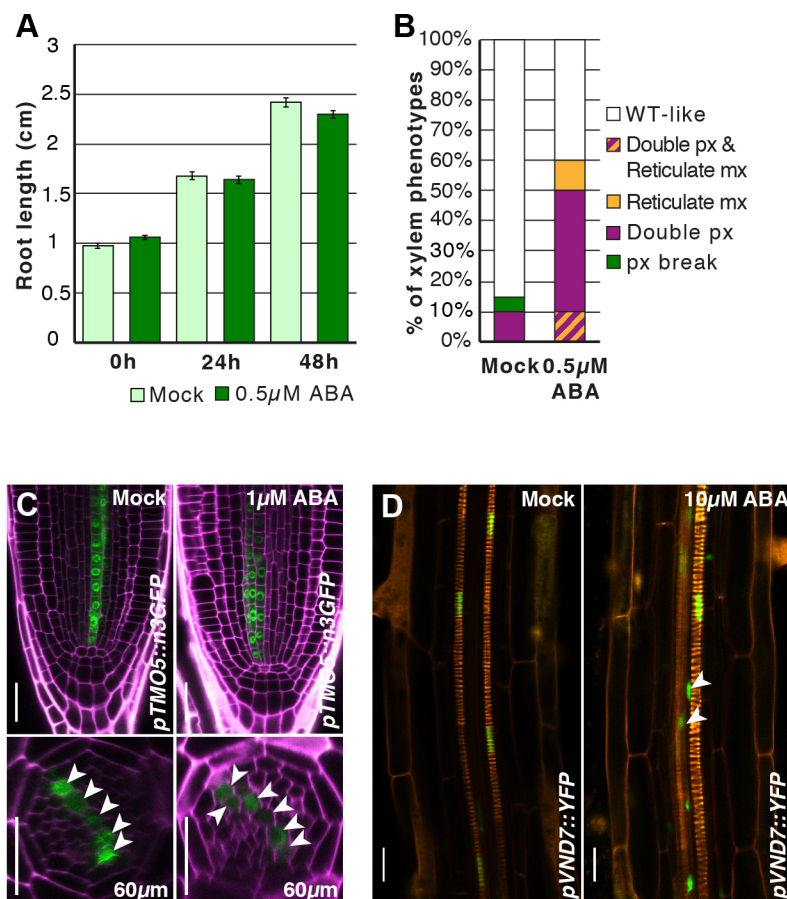


Figure S3. Phenotypic and molecular effects of ABA treatments. **A.** Root lengths after 24h and 48h treatment of wt plants with 0.5 μ M ABA (n=50). Error bars indicate SEM. **B.** Quantification of xylem phenotype appearing after 24h 0.5 μ M ABA (n=20) and mock (n=20) treatments. **C.** Visualization of the xylem identity marker, *pTMO5::n3GFP* after 1 μ M ABA treatment for 48h. White arrows indicate the xylem precursor cells marked by *TMO5* expression. **D.** Visualization of *pVND7::YFP* expression after 10 μ M ABA treatment for 10h. White arrows indicate ectopic *VND7* expression. Scale bars in C and D: 25 μ m.

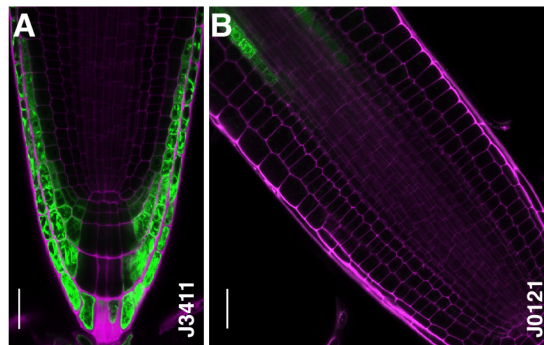


Figure S4. UAS-enhancer trap lines J3411 and J0121. Activation domains of J3411 (**A**) and J0121 (**B**) enhancer trap lines. Scale bars: 25 μ m.

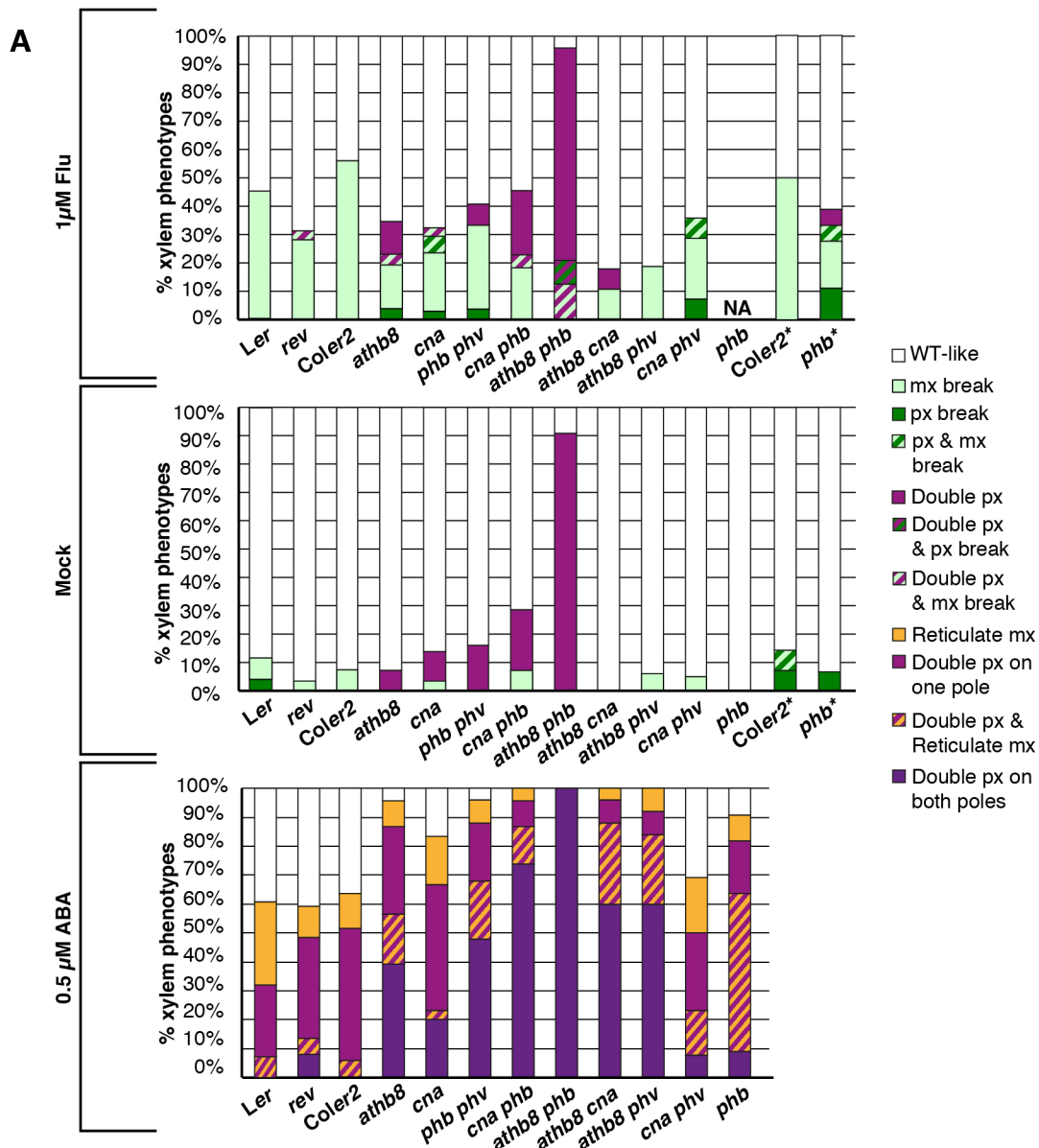


Figure S5. Effects of Flu and ABA treatments on wt and *HD-ZIP III* mutants. Quantification of xylem phenotypes in *HD-ZIP III* mutants after 72h 1μM Flu treatment (**Top panel**) (*Coler2**, n=12; *phb**, n=18; *Coler2*, n=25; *athb8*, n=26; *cna*, n=34; *phb phv*, n=27; *cna phb*, n=22; *athb8 phb*, n=24; *athb8 cna*, n=28; *athb8 phv*, n=32; *cna phv*, n=27; *Ler*, n=31 and *rev6*, n=32), mock treatment (**Middle panel**) (*Coler2**, n=14; *phb**, n=15; *Coler2*, n=27; *athb8*, n=28; *cna*, n=29; *phb phv*, n=25; *cna phb*, n=28; *athb8 phb*, n=22; *athb8 cna*, n=20; *athb8 phv*, n=33; *cna phv*, n=20; *Ler*, n=28 and *rev6*, n=30), and 72h 0.5μM ABA treatment (**Bottom panel**) (*Coler2*, n=33 ABA; *phb*, n=11; *athb8*, n=23; *cna*, n=30; *phb phv*, n=25; *cna phb*, n=25; *athb8 phb*, n=21; *athb8 cna*, n=25; *athb8 phv*, n=25; *cna phv*, n=26; *Ler*, n=29 and *rev6*, n=37). * indicates an independent experiment.

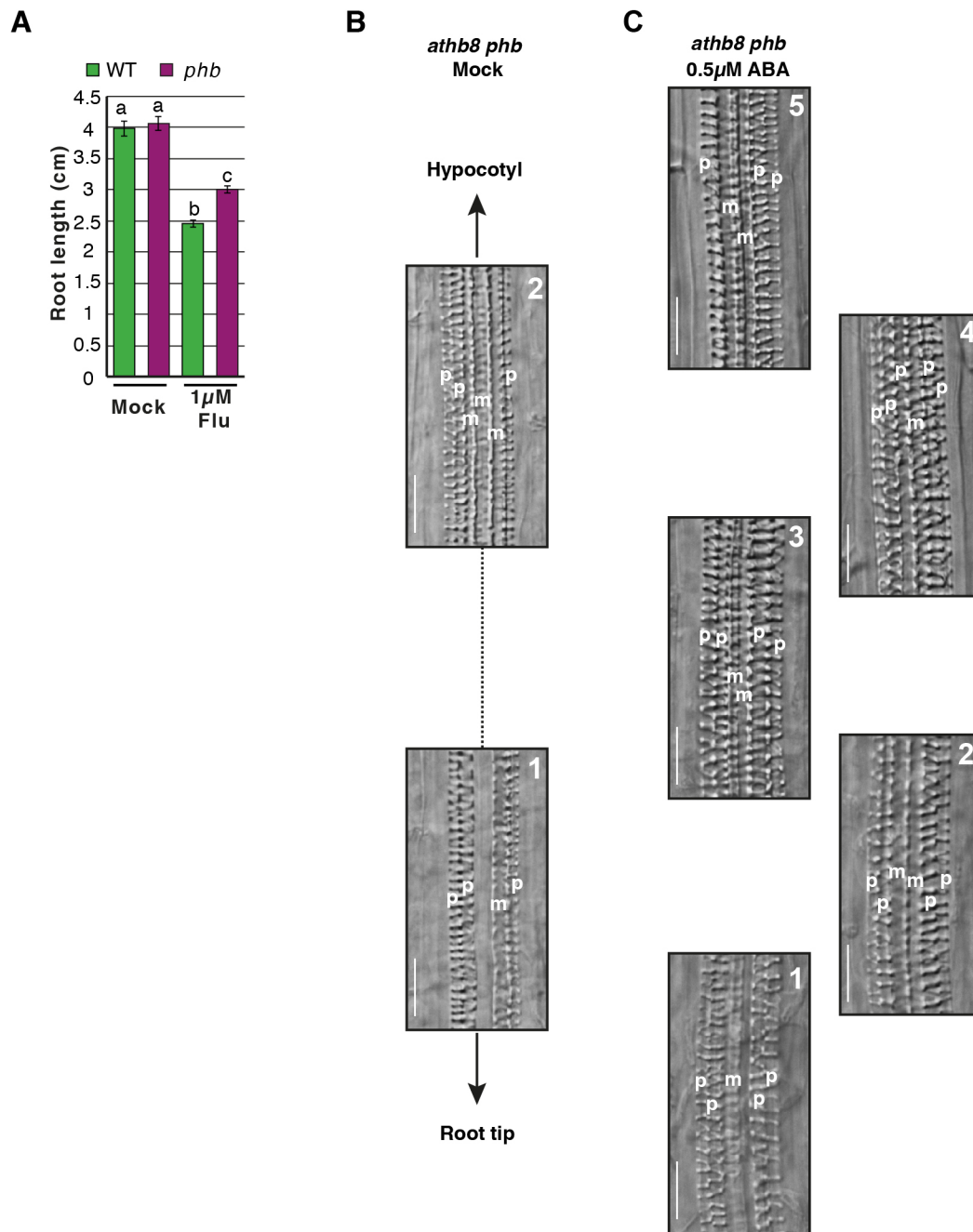


Figure S6. Effect on *HD-ZIP III* mutant root length and xylem phenotypes by Flu and ABA treatments. **A.** Root length of wt and *phb-13* after 1 μ M Flu treatment for 72h (wt mock, n=41; wt Flu, n=59; *phb-13* mock, n=40; *phb-13* Flu, n=48). a, b and c represent significant differences by Tukey's pairwise comparison. **B and C.** Phenotype of *athb8 phb* after mock and ABA treatment. Because *athb8 phb* displays double protoxylem (Carlsbecker et al., 2010) similar to what is seen upon ABA treatment, we categorised the double protoxylem phenotype as either double protoxylem in one pole or in both poles. In wt, 0.5 μ M ABA treatment resulted in double protoxylem in only one of the xylem poles at a given region of the root (Fig. S1D). We considered the appearance of double protoxylem in both xylem poles as an enhancement of the phenotype and quantified the vascular phenotypes in *HD-ZIP III* mutants. Under mock conditions, *athb8 phb* generally displays double protoxylem strands in one of the poles (**B**). However, upon ABA (**C**) double protoxylem strands was formed in both poles in all roots analysed (1,2,3 and 4; Fig. S1D), resembling higher order *HD-ZIP III* loss-of-function mutants (Carlsbecker et al., 2010).

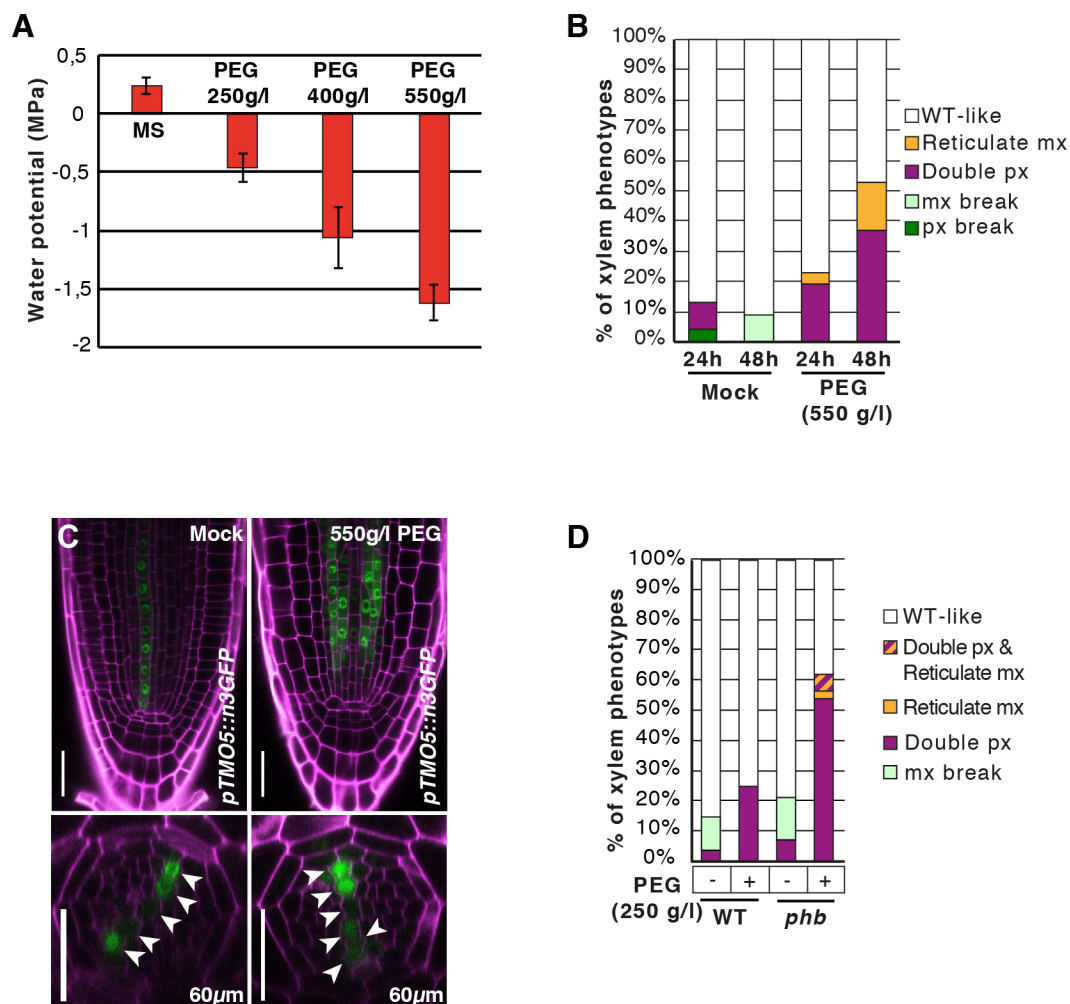


Figure S7. Effects of PEG treatments on wt and *HD-ZIP III* mutants. **A.** Water potentials of media overlaid with different concentrations of PEG. **B.** Frequency of xylem phenotypes occurring after 24 (n=26) and 48h (n=19) of PEG treatment. **C.** Visualization of *pTMO5::n3GFP* after mock and 550g/l PEG treatments for 48h. White arrows indicate the xylem precursor cells marked by *TMO5* expression. **D.** Response of *phb* mutants to low water potential conditions (wt mock, n=27; wt PEG, n=40; *phb* mock, n=28; *phb* PEG, n=37).

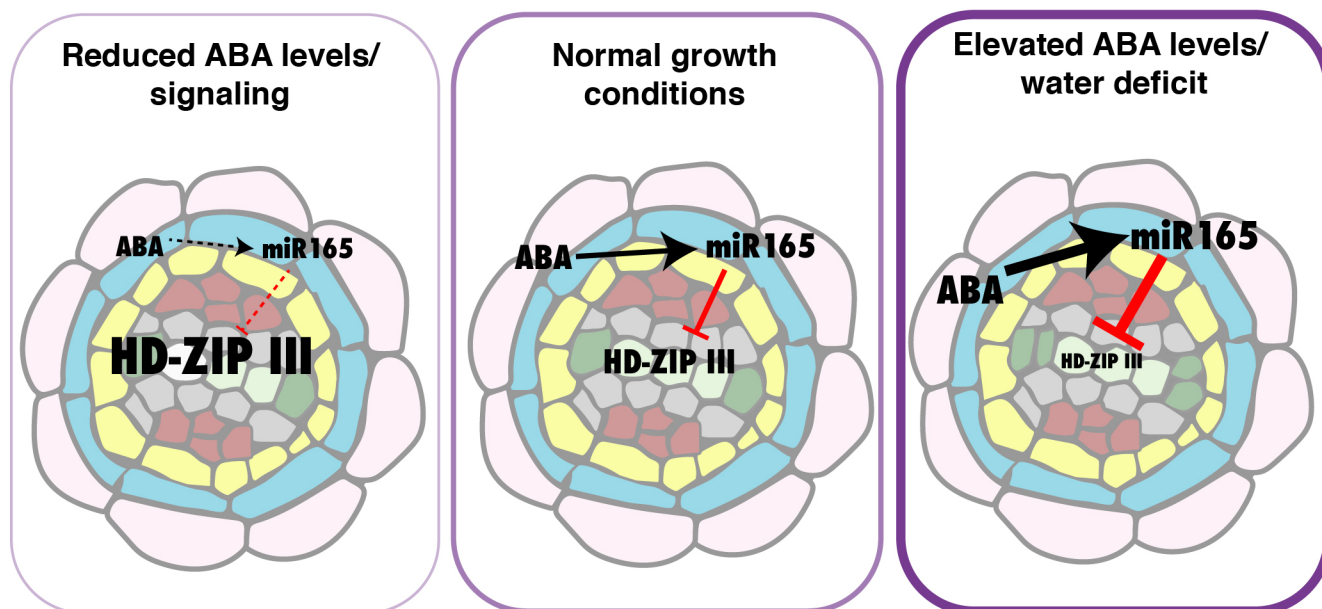


Figure S8. Model depicting the influence of ABA levels on xylem patterning. At optimal ABA levels, the xylem consists of metaxylem flanked by one protoxylem strand on either side. Under reduced ABA level or signalling conditions, *MIR165A* expresses at a lower level than under optimal conditions allowing increased transcript levels of certain HD-ZIP III TFs, and discontinuous xylem strands forms. When ABA levels increase during water limiting conditions, *MIR165A* expression is enhanced, and consequently transcript levels of HD-ZIP III TFs are reduced, resulting in the formation of double protoxylem strands, a phenotype reminiscent of loss of function *HD-ZIP III* mutants.

Supplemental Table S1. Primer sequences used in this study.

ATG	primer name	sequence (5'-3')	use
AT1G27450	APT1 qF	GTTGCAGGTGTTGAAGCTAGAGGT	qPCR
AT1G27450	APT1 qR	TGGCACCAATAGCCAACGCAATAG	qPCR
AT2G34710	PHB qF	CTACTCCGAACGGTGCACTCTG	qPCR
AT2G34710	PHB qR	GTTACAGCCATTGCGGTCGGC	qPCR
AT5G60690	REV qF ex-ex	GCAAGTCGAGGCTCTTGAGCGT	qPCR
AT5G60690	REV qR ex-ex	TCTCGACACCTGCCGTTCTGA	qPCR
AT1G52150	CNA qF	ATTGGCATCTCAAATCCTCAGAGA	qPCR
AT1G52150	CNA qR	GGCAACACGTTTCATAACTTCAACAGC	qPCR
AT4G32880	ATHB8 qF	AACACCACTTGACCCCTCAACATCAG	qPCR
AT4G32880	ATHB8 qR	CACGCAACCAACAAGGCTTATCC	qPCR
AT1G30490	PHV qF	GACCAAAAAACAATCCGAATGA	qPCR
AT1G30490	PHV qR	AATCGGTTTTGGTGGAACCAT	qPCR
AT1G13440	GAPDH qF	ATCAAGAAGGCCATCAAGGA	qPCR
AT1G13440	GAPDH qR	CCTCAGTGTATCCAAAATTCC	qPCR/cDNA synthesis
	miR165-stem loop RT	GTCGTATCCAGTGCAGGGTCCGAGGTATTCGCACTGGATACGACGGGGGA	qPCR/cDNA synthesis
	miR165 F	TCGCTTCGGACCAAGGCTTCA	qPCR
	Universal Reverse	GTGCAGGTCCTCGAGGT	qPCR